Excited-state absorption in $BaY_2F_8:Nd^{3+}$

S. Guy, M. F. Joubert, and B. Jacquier
Laboratoire de Physico-Chimie des Matériaux Luminescents, Université Claude Bernard Lyon I, Bâtiment 205, 43 Boulevard du 11-11-1918, 69622, Villeurbanne CEDEX, France

M. Bouazaoui
Laboratoire de Spectroscopie Hertzienne, Université des Sciences et Technologies Lille I, Bâtiment P5, 59655 Villeneuve d'Ascq, France

(Received 13 November 1992)

Upconversion pumping with yellow cw and pulsed dye lasers was used to produce uv and blue light arising from deexcitation of the $^4D_{3/2}$ and $^2P_{3/2}$ states of Nd^{3+} ions in $BaY_2F_8:Nd^{3+}$. Upconversion excitation occurs via sequential two-photon absorption, which was probed by the anti-Stokes emission dynamics and by a two-color laser experiment. An analysis of the steady-state populations as a function of pumping rates R_1 and R_2 for the two-step excitation is developed. When the excitation frequency is resonant with the $^4F_{3/2} \rightleftharpoons {}^4D_{3/2}$ excited-state absorption transition, the power dependence of the anti-Stokes fluorescence intensity, plotted on a logarithmic scale, shows a straight line with a slope of 1.8. This behavior is explained quite well by the model for a mean-excitation-power regime where the second step is 4 orders of magnitude more efficient than the ground-state absorption.

I. INTRODUCTION

In rare-earth-doped insulators, the main phenomena leading to upconversion-pumped fluorescence, i.e., a fluorescence that occurs at a wavelength shorter than the wavelength of the excitation source, may be summarized as follows.

(1) Excited-state absorption: This is a single-ion process. One photon of energy E_1 is absorbed, after which another photon of energy E_2 generates a transition from a metastable state 2 to a higher energy level. The energy of the final state 3 is, at most, equal to the sum of the two-photon energies. The anti-Stokes fluorescence decay characterizes only the relaxations of state 3.

(2) Direct two-photon absorption: This is also a single-ion process in which two photons of energies E_1 and E_2 are simultaneously absorbed through a virtual intermediate quantum state. The energy of the final state 3 is equal to E_1+E_2. As in the previous case, the anti-Stokes fluorescence decay characterizes only the relaxations of state 3.

(3) Energy transfer: Two kinds of energy transfer are considered here; cross relaxation between ions in their excited states (the energy absorbed by the donor is transferred to the acceptor, which is already in an excited state), and cooperative sensitization (the energy accumulated by two excited ions is transferred to a third ion). Now the time dependence of the anti-Stokes fluorescence, which may be calculated using rate equations, does not depend only on the final-state relaxations but also on the relaxation rates of the intermediate states, on the energy-transfer probability, ...

These processes are basically nonlinear. They have been discussed by Auzel[1] who showed that excited-state absorption and energy transfer are usually much more probable by about 10 orders of magnitude than the direct two-photon absorption. The cross sections for direct two-photon absorption are too low to permit effective pumping of a laser. This is why all the rare-earth-doped solid-state upconversion lasers (i.e., optically pumped lasers that oscillate at frequencies higher than those used for pumping) mentioned in the literature are pumped via excited-state absorption or energy-transfer processes. More than two-step successive photon absorptions or energy transfers have been achieved in some specific cases. Among these lasers, $LaF_3:Nd^{3+}$ (Ref. 2) and $LiYF_4:Nd^{3+}$ (Ref. 3) show a reasonable efficiency but unfortunately operation is restricted to low temperatures. However, they behave in a different way as far as exited-state dynamics is concerned. Our goal is to study other trivalent neodymium doped fluorides with a view to their application as solid-state upconversion lasers, which may operate at room temperature.

In this paper, we report on the first observation of uv and blue upconversion-pumped fluorescence in $BaY_2F_8:Nd^{3+}$. Section II describes crystallographic and optical properties of $BaY_2F_8:Nd^{3+}$ as well as laser techniques used in this study. The experimental results are presented in Sec. III and a theoretical interpretation is given in Sec. IV in terms of exited-state absorption. Some conclusions and future plans are drawn in Sec. V.

II. MATERIAL AND EXPERIMENTAL EQUIPMENT

The two $BaY_2F_8:Nd^{3+}$ samples used in this study were grown by the Czochralski technique at the MIT crystal-growth laboratory, and contained, respectively, 0.4 and 1 at. % Nd^{3+}. For the spectroscopic measurements, we cut and polished thin plates of a few millimetercubes, which were cooled to indicate temperatures in a liquid-helium optical cryostat with a heating gas system and a regulator

allowing the temperature to be varied between 1.6 and 300 K.

A. Material

The crystal structure of BaY_2F_8 was investigated by Kaminskii *et al.*[4] and the space group was determined to be $C_{2/m}$ with crystallographic parameters $a=6.972$ Å, $b=10.505$ Å, and $c=4.260$ Å. There are two formulas per unit cell, and 1.28 10^{22} yttrium ions/cc. The rare-earth ions incorporated in this host are surrounded by 8 fluoride anions and occupy crystallographic sites of C_2 symmetry. In BaY_2F_8:Nd^{3+}, the Nd^{3+} energy levels are Kramers' doublets belonging to the $(\Gamma_3+\Gamma_4)$ irreducible representation of the C_2 double group. This results in $J+\frac{1}{2}$ components for each J level where J is a half odd integer. All the transitions between these Kramers' doublets are allowed and there are no selection rules predicting completely polarized optical transitions. In a recent paper,[5] absorption and fluorescence measurements at low temperature were used to obtain an energy-level scheme for the Stark components of the Nd^{3+} manifolds in BaY_2F_8 up to 40 000 cm^{-1} (see Fig. 1) and the fluorescence lifetimes of the $^4F_{3/2}$, $^2P_{3/2}$, $^4D_{3/2}$, and $^2F(2)_{5/2}$ levels were measured between liquid-helium and room temperatures.

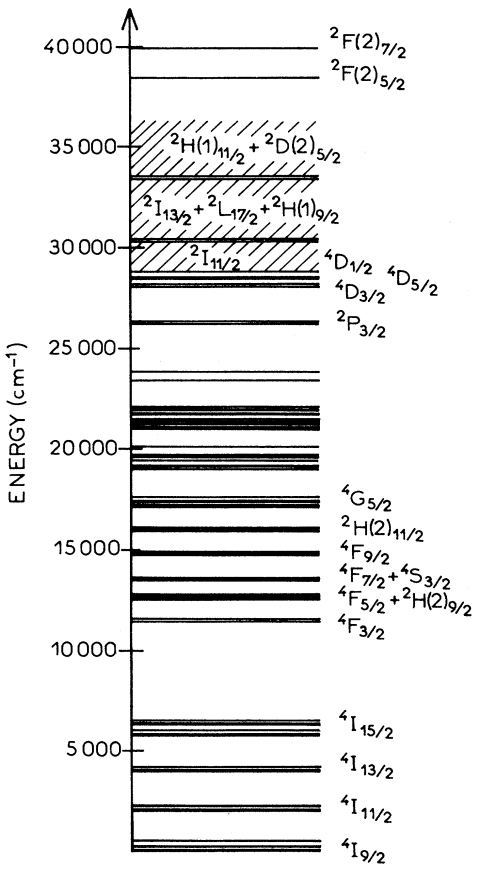

FIG. 1. Energy level scheme for the Nd^{3+} Stark components in BaY_2F_8:Nd^{3+}.

B. Pulsed laser excitation equipment

Laser excitation was achieved by one or two home made dye lasers pumped by a frequency doubled Quantel model 481 infrared YAG:Nd^{3+} laser (pulse length, 10 ns; repetition rate, 10 Hz, and energy per pulse, up to 350 mJ at 5320 Å). The laser beam wavelength was analyzed by a home made lambdameter (resolution: 0.05 Å). The anti-Stokes emission was collected at 90° to the laser beam direction and analyzed by a $\frac{1}{4}$m Jarrel Ash monochromator followed by a Hamamatsu R955 photomultiplier and a Lecroy 3521 multichannel analyzer. This experimental setup was controlled by a PC.

C. Continuous laser excitation equipment

Laser excitation was achieved by a Spectra Physics model 380 ring dye laser pumped by a cw coherent 10 W argon laser. The wavelength of the excitation laser beam was analyzed by a Jobin Yvon HRS1 monochromator with a dispersion of 12 Å/mm followed by a Hamamatsu R955 photomultiplier connected to a Lecroy 9410 digital oscilloscope. The laser beam was chopped and focused on the sample. The infrared $^4F_{3/2}$ fluorescence and the violet $^2P_{3/2}$ anti-Stokes emission were collected simultaneously at 90° to the laser beam direction. The infrared fluorescence was analyzed by a Jobin Yvon H25 monochromator and detected by a cooled ADC403L germanium cell. The ultraviolet emission was analyzed by a $\frac{1}{4}$ m Jarrel Ash monochromator followed by a EMI 6256S photomultiplier. These two signals were sent to lock-in amplifiers. This experimental setup was controlled by a PC.

III. EXPERIMENTAL RESULTS

In this section, we present the first investigation of the anti-Stokes fluorescence of neodymium in BaY_2F_8:0.4 at % Nd^{3+} observed at liquid-helium temperature.

A. Pulsed laser excitation

The laser beam (several tens of μJ/pulse) was focused on the sample with a 250 mm focal lens. Pulsed laser excitation was performed between 5750 and 6270 Å. After selective excitation at 5805.5 Å (one of the $^4I_{9/2} \Longrightarrow {}^4G_{5/2}$ transitions), the blue and ultraviolet anti-Stokes emissions are due to transitions $^4D_{3/2} \Longrightarrow {}^4I_{9/2,11/2,13/2,15/2}$ and $^2P_{3/2} \Longrightarrow {}^4I_{9/2,11/2,13/2,15/2}$. The relative intensities of these emissions are exactly the same as those obtained after selective excitation in one of the Stark components of the $^4D_{3/2}$ manifold.[5] The excitation spectrum of the line located at 3573 Å ($^4D_{3/2} \Longrightarrow {}^4I_{9/2}$) is presented in Fig. 2. The three lines located at 5780, 5805.5, and 5829 Å are assigned to the $^4I_{9/2} \Longrightarrow {}^4G_{5/2}$ transitions, while the two lines located at 6205.3 and 6229.1 Å correspond to some components of the transition $^4I_{9/2} \Longrightarrow {}^2H(2)_{11/2}$ (see the Table I of Ref. 5). The excitation line located at 6038 Å is attributed to the transition between the lower Stark components of the $^4F_{3/2}$ and $^4D_{3/2}$ manifolds; in this case the laser frequency is not resonant with any of the absorption transitions from the ground state to any of the

levels above $^4F_{3/2}$, so the excited-state absorption rate from $^4F_{3/2}$ and $^4D_{3/2}$ must be relatively high.

We have recorded the decay of this anti-Stokes emission at 3573 Å. At all the reported above excitation wavelengths, the decay is exponential with a time constant of 4.2 μs, which is identical to the one measured after selective excitation in one of the Stark components of the $^4D_{3/2}$ manifold.[5] The absence of rise time and the fact that this anti-Stokes fluorescence decay characterizes only the upper emitting level suggests that the mechanism responsible to this emission is an excited-state absorption process.

In the excitation spectrum presented in Fig. 2(a), the central peak is composed of two lines: a broad one located at 5805.5 Å, unambiguously attributed to one of the $^4I_{9/2} \rightleftharpoons {}^4G_{5/2}$ transitions,[5] and another one, sharper and located at 5807.6 Å, which does not correspond to any electronic absorption transition from the ground state. The only explanation we can propose is that this line may be related to an excited-state resonance as for the excitation line at 6038 Å. In that case, a two laser beam excitation experiment with one beam λ_1 centered at 5805.5 Å and the second beam λ_2 tunable from 5800 to 5812 Å should enhance the 5807.6 Å excitation line compared to the other one. The two laser beam intensities are chosen sufficiently low to avoid any detectable anti-Stokes emission when only one of the two lasers is switched on. The excitation spectrum recorded with the two laser beams focused on the sample is presented in Fig. 3. The peak at 5807.6 Å is much more intense than the other one, giving proof of the validity of the interpretation. In this material, due to the absence of knowledge of all the Stark components of the Nd^{3+} manifolds located above $^4D_{5/2}$, we did not assign this excited state resonance at 5807.6 Å (17 219 cm^{-1}). By looking at the Nd^{3+} energy level scheme in other fluorides as $LiYF_4:Nd^{3+}$ (Ref. 6) or $LaF_3:Nd^{3+}$ (Ref. 7), this frequency may match several excited-state transitions as a $^4F_{3/2}$, $^4F_{5/2}+2H(2)_{9/2} \rightleftharpoons {}^2I_{11/2}$ or $^4F_{7/2}+{}^4S_{3/2}$, $^4F_{9/2}$, $^2H(2)_{11/2} \rightleftharpoons {}^2I_{13/2}+{}^2L_{17/2}+{}^2H(1)_{9/2}$ or $^4G_{5/2} \rightleftharpoons {}^2H(1)_{11/2}+{}^2D(2)_{5/2}$. A run of two laser beam excitation experiments is under consideration to clarify this point.

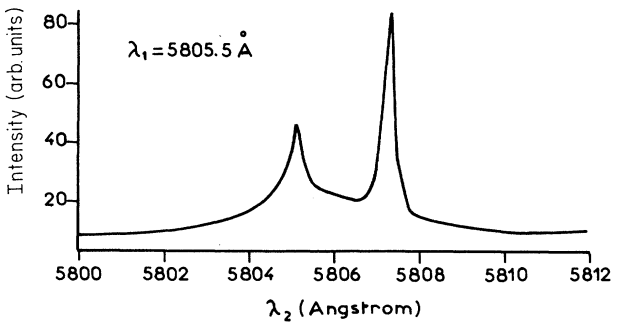

FIG. 3. Two laser beam excitation spectrum of the ultraviolet (3573 Å) fluorescence of BaY_2F_8:0.4 at.% Nd^{3+} at 6 K.

B. Continuous laser excitation

The experimental results discussed in this section concern the crystal with 0.4 at.% Nd^{3+}. Some experiments were carried out with the 1 at.% sample leading to similar qualitative results. After excitation around 5800 Å ($^4I_{9/2} \rightleftharpoons {}^4G_{5/2}$) and also after excitation around 6038 Å ($^4F_{3/2} \rightleftharpoons {}^4D_{3/2}$), the cw excitation spectra of the 4143 Å anti-Stokes fluorescence line related to one of the $^2P_{3/2} \rightleftharpoons {}^4I_{11/2}$ transitions were analyzed. Simultaneously, we have detected the infrared $^4F_{3/2} \rightleftharpoons {}^4I_{9/2}$ emission located at 8752 Å.

1. Excitation into the $^4G_{5/2}$ level

The laser beam was focused on the sample with a 100 mm focal lens. The excitation spectra of the blue anti-Stokes fluorescence and of the infrared Stokes emission were recorded with different excitation powers: 190 mW focused on the sample, 40 mW focused on the sample, and 40 mW without focusing the beam to get a very low excitation density. These excitation spectra are presented in Fig. 4 showing the three lines assigned to the $^4I_{9/2} \rightleftharpoons {}^4G_{5/2}$ transitions. By raising the laser excitation density, the intensity of the blue anti-Stokes emission is increased as a consequence of a growing $^2P_{3/2}$ population due to efficient excitated-state absorption. On the other

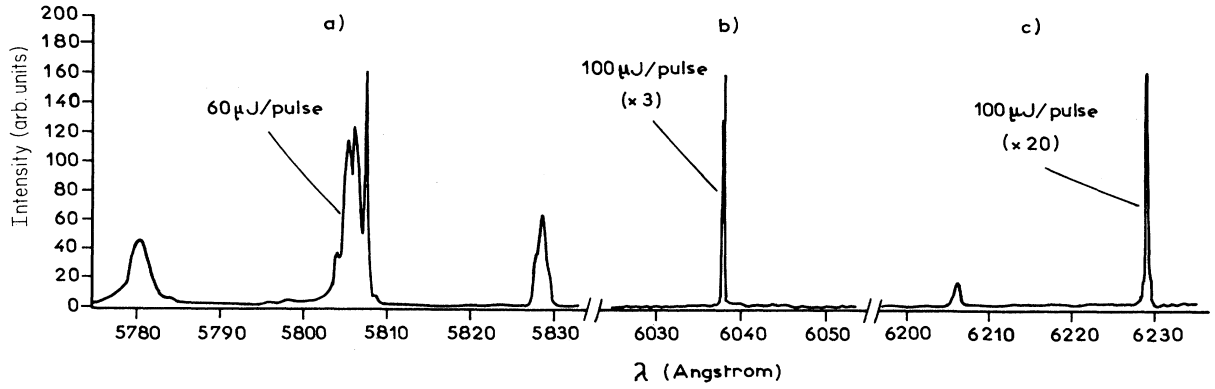

FIG. 2. Excitation spectrum of the ultraviolet (3573 Å) fluorescence of BaY_2F_8:0.4 at.% Nd^{3+} at 6 K.

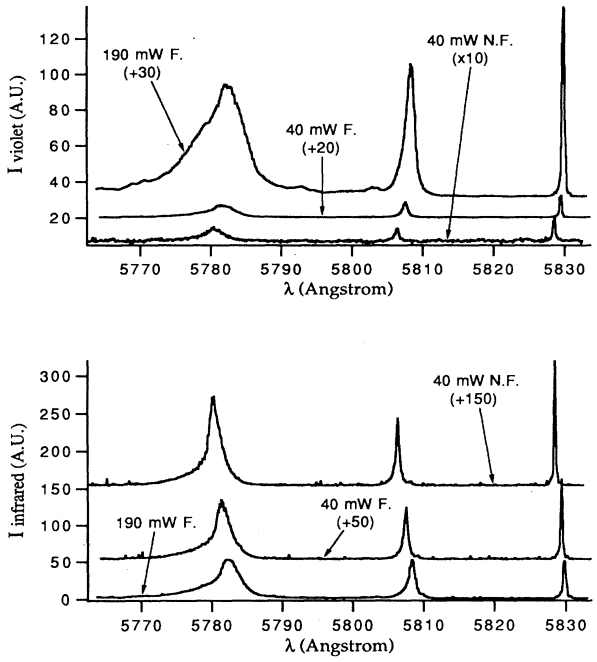

FIG. 4. Excitation spectra of the violet (4143 Å) and infrared (8752 Å) fluorescences of BaY_2F_8:0.4 at.% Nd^{3+} at 6 K.

hand, the intensity of the Stokes infrared fluorescence decreases. These results will be theoretically interpreted in the next section.

2. *Excitation around 6038* Å

Using a laser power of 190 mW and focusing the laser beam on the sample with $f=100$ mm, the excitation spectrum of the anti-Stokes fluorescence (Fig. 5) shows an excitation line located at 6038 Å. It is attributed to the excited-state transition between the lower Stark components of the $^4F_{3/2}$ and $^4D_{3/2}$ manifolds. In this case, the intensity of the 4143 Å emission is much lower than after excitation at 5829 Å (see Fig. 4) and we did not detect any $^4F_{3/2} \Longrightarrow {}^4I_{9/2}$ infrared fluorescence. The power dependence of this anti-Stokes fluorescence is

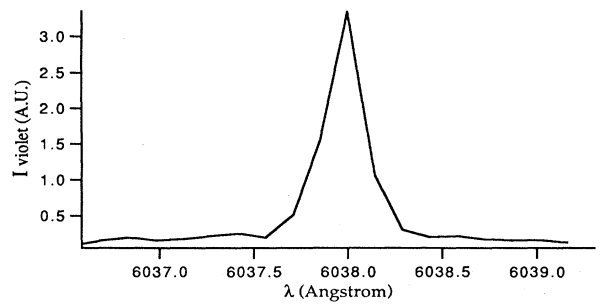

FIG. 5. Excitation spectrum of the violet (4143 Å) fluorescence of BaY_2F_8:0.4 at.% Nd^{3+} at 6 K. The power of the laser beam is 190 mW focused on the sample with $f=100$ mm.

drawn on Fig. 6 on a logarithmic scale, showing a straight line with a slope of 1.8.

IV. DISCUSSION

A. Theoretical background for excited-state absorption

As already mentioned in the Introduction, excited-state absorption is one of the well known mechanisms leading to anti-Stokes fluorescence. Figure 7 shows the general energy scheme of this process. Since the multiphonon relaxations, represented by dotted arrows in Fig. 7, are fast compared to all other processes involved, the system may be reasonably approximated by a three-level system. The excitation process is then described by the following rate equations:

$$\begin{aligned} d(n_1)/dt &= -R_1 n_1 + W_2 n_2 + bW_3 n_3 \ , \\ d(n_2)/dt &= R_1 n_1 - (W_2 + R_2) n_2 + (1-b) W_3 n_3 \ , \\ d(n_3)/dt &= R_2 n_2 - W_3 n_3 \ , \\ n_1 + n_2 + n_3 &= 1 \ , \end{aligned} \qquad \text{(system I)}$$

where n_i is the population of level i. The absorption from the ground state and the excitation via absorption from level 2 are characterized by pumping rates R_1 and R_2. W_2 and W_3 are the relaxation rates of levels 2 and 3, respectively. The branching ratio of the relaxation probabilities of level 3 is described by the parameter b with $(1-b)W_3$ being the decay rate to level 2. These equations can be solved analytically in the long-time or steady-state limit. Using $R_2 = kR_1$, the result is

$$\begin{aligned} n_3^\infty &= \frac{kR_1^2}{kR_1^2 + W_3 R_1 (1+kb) + W_2 W_3} \ , \\ n_2^\infty &= \frac{W_3 R_1}{kR_1^2 + W_3 R_1 (1+kb) + W_2 W_3} \ , \\ n_3^\infty / n_2^\infty &= R_2 / W_3 = t_3 R_2 \ . \end{aligned} \qquad \text{(system II)}$$

This result shows that the power dependence of the steady-state populations is a function of k, the pumping rate ratio. During a single beam two-step excitation experiment, the photon energy may be in resonance either only with the energy of the absorption transition $1 \Longrightarrow 2'$ or only in resonance with the energy of the excited-state absorption $2 \Longrightarrow 3'$, but also in resonance with the two absorption transitions. So, it is clear that the ratio $R_2/R_1 = k$ may have different values. On the other hand, the third equation of system II shows that, whatever the value of the pumping ratio is, the population ratio n_3^∞ / n_2^∞ increases with the excitation density.

B. Application to the case of BaY_2F_8:Nd^{3+}

In the present case, n_1, n_2, and n_3 denote the populations of the $^4I_{9/2}$, $^4F_{3/2}$, and $^2P_{3/2}$ states, respectively. So, in the steady-state limit, the $^2P_{3/2}$ anti-Stokes fluores-

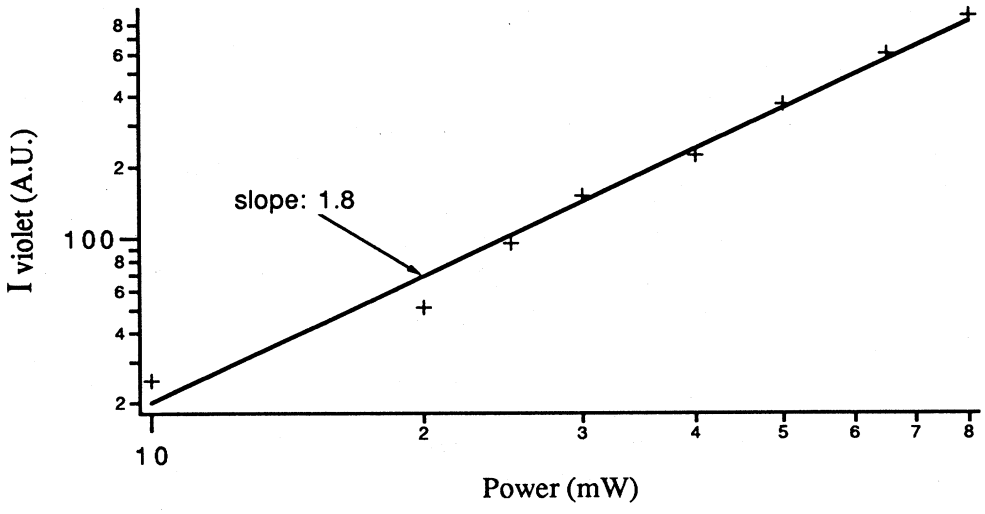

FIG. 6. Logarithmic plot of the experimental (+++) power dependence of the violet (4143 Å) fluorescence of BaY_2F_8:0.4 at.% Nd^{3+} at 6 K. The excitation wavelength is 6038 Å.

cence is proportional to n_3^∞ and the infrared $^4F_{3/2}$ emission is proportional to n_2^∞. The measured values of W_2 and W_3 are, respectively, 1751 s^{-1} and 8621 s^{-1} (Ref. 5) and, as the relative emission intensities in $BaY_2F_8:Nd^{3+}$ are similar to those in $LiYF_4:Nd^{3+}$ (Ref. 8), the b parameter is assumed to be equal to 0.2 as in the case of $LiYF_4:Nd^{3+}$ (Ref. 9).

Figure 8 shows the power dependence of the steady-state populations n_3^∞ and n_2^∞ for different values of k. For these diagrams, the most efficient pumping rate R_2 or R_1 varies from 1000 to 20 000 s^{-1}. We now discuss each of these graphs in turn:

(i) $R_2/R_1=10^4$: This may correspond, for example, to a resonance only between excited states, the first step being an absorption in the vibronic sideband of level 2' [$^2H(2)_{11/2}$ or $^4G_{5/2}$]. In this case, the populations n_3^∞ and n_2^∞ are relatively low and increase with the excitation density. At very low power, the population n_3^∞ is proportional to R_2^2; then for R_2 between 1000 and 10 000 s^{-1}, n_3^∞ is proportional to $R_2^{1.7}$; and at higher intensity, the power dependence of n_3^∞ becomes linear.

(ii) $R_2/R_1=1$: Now the pumping rates are the same and levels 2 ($^4F_{3/2}$) and 3 ($^2P_{3/2}$) get higher populations than in the previous case. At this point, it is very interesting to note that n_2^∞ increase with the excitation power then decreases as soon as R_1R_2 is equal to W_2W_3.

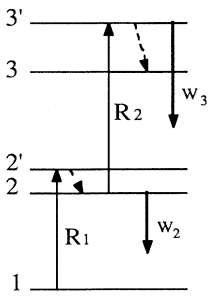

FIG. 7. General energy scheme for excited-state absorption.

(iii) $R_2/R_1=10^{-4}$: This may be the case if the photon energy is in resonance only with the energy of the absorption transition from the ground state. The $^4F_{3/2}$ population n_2^∞ is relatively high and saturates under high excita-

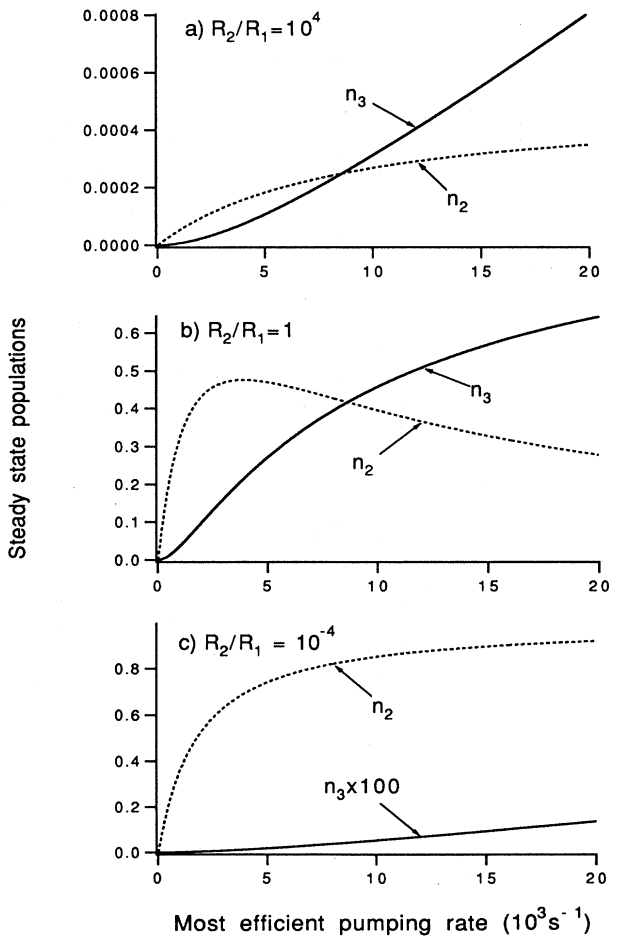

FIG. 8. Calculated power dependence of the steady-state populations n_3^∞ and n_2^∞ for different values of R_2/R_1.

tion density, while the $^2P_{3/2}$ steady-state population n_3^∞ remains very low.

After excitation in one of the $^4G_{5/2}$ Stark components, the fact that increasing the excitation density increases the ratio of the intensity of the blue anti-Stokes emission with respect to the intensity of the infrared fluorescence (see Fig. 4), is in agreement with the third equation of system II. The decrease of the absolute value of the $^4F_{3/2}$ emission indicates that the pumping rates R_2 and R_1 should have about the same value (see Fig. 8).

For $\lambda_{exc}=6038$ Å (perfect resonance only between excited states), R_2 is probably greater than for $\lambda_{exc}=5829$ Å (resonant absorption from the ground state). So, if the observed intensity of the 4143 Å emission is much lower than after excitation at 5829 Å (see Figs. 4 and 5), the $^4F_{3/2} \rightleftharpoons {}^4I_{9/2}$ infrared fluorescence must be extremely weak. Thus, the fact that we could not detect infrared light is not surprising. The experimental power dependence of the anti-Stokes fluorescence drawn on Fig. 6 is in agreement with this theory for a mean-excitation-power regime when $R_2/R_1 \approx 10^4$. Such a pumping rate ratio can be easily achieved in the case of perfect resonance only between excited states.

V. CONCLUSION

We report an observation of uv and blue upconversion-pumped fluorescence in $BaY_2F_8:Nd^{3+}$ coming from the Nd^{3+} $^2P_{3/2}$ and $^4D_{3/2}$ manifolds after excitation in the yellow spectral range. After pulsed laser excitation, the anti-Stokes emission dynamics show that the principal mechanism for generating this fluorescence is a sequential two-step absorption. In some cases, the laser frequency is in resonance with the ground-state absorption ($^4I_{9/2} \rightleftharpoons {}^4G_{5/2}$ or $^4I_{9/2} \rightleftharpoons {}^2H(2)_{11/2}$), but sometimes the exciting laser is resonant only with the excited-state absorption transition as confirmed by a two-color laser experiment. At this point, some comparisons may be drawn with other Nd^{3+}-doped fluoride crystals. First, the cw yellow excitation ($^4I_{9/2} \rightleftharpoons {}^4G_{5/2}$) of the anti-Stokes fluorescence is very efficient, confirming that the doubly resonant pumping scheme demonstrated in the $LaF_3:Nd^{3+}$ upconversion laser[2] should also operate with $BaY_2F_8:Nd^{3+}$, as was previously suggested.[5] Second, this anti-Stokes fluorescence is also observed using single excitation laser frequency resonant only with the $^4F_{3/2} \rightleftharpoons {}^4D_{3/2}$ excited-state absorption transition. Nevertheless, such an excitation process is much less efficient than in $LiYF_4:Nd^{3+}$ where an avalanche mechanism was demonstrated.[9] In this avalanche process, a cross relaxation energy transfer from a state in which one Nd^{3+} ion is in $^2P_{3/2}$ and one in the $^4I_{9/2}$ ground state leads to two ions in the intermediate $^4F_{3/2}$ state and thus to a feedback mechanism for enhanced resonant absorption of the pump light and excitation of $^2P_{3/2}$. In $BaY_2F_8:Nd^{3+}$ there is no energy gap coincidence for such cross relaxation process and the experimental results (time or power dependence of the anti-Stokes or Stokes emission) are well described with a simple excited-state absorption model. The theory developed in this study clearly shows the dependence of the Stokes and anti-Stokes fluorescences on the ratio of the pumping rates R_1 and R_2 for the two-step excitation. As a matter, the model reproduces quite well the linear dependence very often observed in upconversion-pumped solid state lasers.[2,10,11]

We also observed an anti-Stokes fluorescence arising from deexcitation of the $^2F(2)_{5/2}$ state of Nd^{3+} after resonant excitation in one of the Stark components of the $^4D_{3/2}$ or $^2P_{3/2}$ states of Nd^{3+}. These results will be described and interpreted in the future.

ACKNOWLEDGMENTS

We thank A. Cassanho of the Center for Materials Science and Engineering, MIT, for providing the crystals used in this study. We also acknowledge R. M. Macfarlane of the Almaden Research Center, IBM, for helpful discussions. Laboratoire de Physico Chimie des Matériaux Luminescents is Laboratoire Unité de Recherche Associée au CNRS No. 442.

[1] F. Auzel, in *Radiationless Processes*, edited by B. DiBartolo (Plenum, New York, 1979), p. 213.
[2] R. M. Macfarlane, Appl. Phys. Lett. **52**, 1300 (1988).
[3] F. Tong, R. M. Macfarlane, and W. Length (unpublished).
[4] A. A. Kaminsii, B. P. Sobolev, S. E. Sarkisov, G. A. Denisenko, V. V. Ryabchenov, V. A. Federov, and T. V. Uranova, Izv. Akad. Nauk SSSR, Neorg. Mater. **18**, 482 (1982).
[5] M. F. Joubert, B. Jacquier, C. Linarès, and R. M. Macfarlane, J. Lumin. **47**, 269 (1991).
[6] C. Görller-Walrand, L. Fluyt, P. Porcher, A. A. S. Da Gama, G. F. De Sa, W. T. Carnall, and G. L. Goodman, J. Less-Common Met. **148**, 339 (1989).
[7] W. T. Carnall, H. Crosswhite, and H. M. Crosswhite (unpublished).
[8] M. F. Joubert, B. Jacquier, C. Linarés, and R. M. Mcfarlane, J. Lumin. **53**, 477 (1992).
[9] W. Lenth and R. M. Macfarlane, J. Lumin. **45**, 346 (1990).
[10] J. Y. Allain, M. Monerie, and H. Poignant, Electron. Lett. **26**, 261 (1990).
[11] S. G. Grubb, K. W. Bennett, R. S. Cannon, and W. F. Humer (unpublished).